

This is the accepted manuscript made available via CHORUS. The article has been published as:

## Ground-state degeneracy in the Levin-Wen model for topological phases

Yuting Hu, Spencer D. Stirling, and Yong-Shi Wu

Phys. Rev. B **85**, 075107 — Published 7 February 2012

DOI: [10.1103/PhysRevB.85.075107](https://doi.org/10.1103/PhysRevB.85.075107)

# Ground State Degeneracy in the Levin-Wen Model for Topological Phases

Yuting Hu,<sup>1,\*</sup> Spencer D. Stirling,<sup>1,2,†</sup> and Yong-Shi Wu<sup>3,1,‡</sup>

<sup>1</sup>*Department of Physics and Astronomy, University of Utah, Salt Lake City, UT 84112, USA*

<sup>2</sup>*Department of Mathematics, University of Utah, Salt Lake City, UT 84112, USA*

<sup>3</sup>*Department of Physics and Center for Field Theory and Particle Physics, Fudan University, Shanghai 200433, China*

(Dated: January 24, 2012)

We study properties of topological phases by calculating the ground state degeneracy (GSD) of the 2d Levin-Wen (LW) model. Here it is explicitly shown that the GSD depends only on the spatial topology of the system. Then we show that the ground state on a sphere is always non-degenerate. Moreover, we study an example associated with a quantum group, and show that the GSD on a torus agrees with that of the doubled Chern-Simons theory, consistent with the conjectured equivalence between the LW model associated with a quantum group and the doubled Chern-Simons theory.

PACS numbers: 05.30.Pr 71.10.Hf 02.10.Kn 02.20.Uw

## I. INTRODUCTION

In recent years two-dimensional topological phases have received growing attention from the science community. They represent a novel class of quantum matter at zero temperature whose bulk properties are robust against weak interactions and disorders. Topological phases may be divided into two families: *doubled* (with time-reversal symmetry, or TRS, preserved), and *chiral* (with TRS broken). Either type may be exploited to do fault-tolerant (or topological) quantum computing<sup>1-4</sup>.

*Chiral* topological phases were first discovered in integer and fractional quantum Hall (IQH and FQH) liquids. Mathematically, their effective low-energy description is given by Chern-Simons theory<sup>5</sup> or (more generally) topological quantum field theory (TQFT)<sup>6</sup>. One characteristic property of FQH states is ground state degeneracy (GSD), which depends only on the spatial topology of the system<sup>7-9</sup> and is closely related to fractionization<sup>10-12</sup> of quasiparticle quantum numbers, including fractional (braiding) statistics<sup>13,14</sup>. In some cases the GSD has been computed in refs.<sup>12,15</sup>.

Chern-Simons theories are formulated in the continuum and have no lattice counterpart. Doubled topological phases, on the other hand, do admit a discrete description. The first known example was Kitaev's toric code model<sup>1</sup>.

More recently, Levin and Wen (LW)<sup>16</sup> constructed a discrete model to describe a large class of doubled phases. Their original motivation was to generate ground states that exhibit the phenomenon of string-net condensation<sup>17</sup> as a physical mechanism for topological phases. The LW model is defined on a trivalent lattice (or graph) with an exactly soluble Hamiltonian. The ground states in this model can be viewed as the fixed-point states of some renormalization group flow<sup>18,19</sup>. These fixed-point states look the same at all length scales and have no local degrees of freedom.

The LW model is believed to be a Hamiltonian version of the Turaev-Viro topological quantum field theory (TQFT) in three dimensional spacetime<sup>4,20,21</sup> and, in particular cases, discretized version of *doubled* Chern-

Simons theory<sup>22,23</sup>. Like Kitaev's toric code model<sup>1</sup>, we expect that the subspace of degenerate ground states in the LW model can be used as a fault-tolerant code for quantum computation.

In this paper we report the results of a recent study on the GSD of the LW model formulated on a (discretized) closed oriented surface  $M$ . Usually the GSD is examined as a topological invariant<sup>20,21,23</sup> of the 3-manifold  $S^1 \times M$ . In a Hamiltonian approach accessible to physicists, we will explicitly demonstrate that the GSD in the LW model depends only on the topology of  $M$  on which the system lives and, therefore, is a topological invariant of the surface  $M$ . We also show that the ground state of any LW Hamiltonian on a sphere is always non-degenerate. Moreover, we examine the LW model associated with quantum group  $SU_k(2)$ , which is conjectured to be equivalent to the doubled Chern-Simons theory with gauge group  $SU(2)$  at level  $k$ , and compute the GSD on a torus. Indeed we find an agreement with that in the corresponding doubled Chern-Simons theory<sup>6,24</sup>. This supports the above-mentioned conjectured equivalence between the doubled Chern-Simons theory and the LW model, at least in this particular case.

The paper is organized as follows. In Section II we present the basics of the LW model, easy to read for newcomers. In Section III topological properties of the ground states are studied, and the topological invariance of their degeneracy is shown explicitly. In section IV we demonstrate how to calculate the GSD in a general way. In section V we provide examples for the calculation particularly on a torus. Section VI is devoted to summary and discussions. The detailed computation of the GSD is presented in the appendices.

## II. THE LEVIN-WEN MODEL

Start with a fixed (connected and directed) trivalent graph  $\Gamma$  which discretizes a closed oriented surface  $M$  (such as a torus). To each edge in the graph we assign a string type  $j$ , which runs over a finite set  $j = 0, 1, \dots, N$ . Each string type  $j$  has a "conjugate"  $j^*$  that describes

the effect of reversing the edge direction. For example  $j$  may be an irreducible representation of a finite group or (more generally) a quantum group<sup>25</sup>.

Let us associate to each string type  $j$  a quantum dimension  $d_j$ , which is a positive number for the Hamiltonian we define later to be hermitian. To each triple of strings  $\{i, j, k\}$  we associate a *branching rule*  $\delta_{ijk}$  that equals 1 if the triple is “allowed” to meet at a vertex, 0 if not (in representation language the tensor product  $i \otimes j \otimes k$  either contains the trivial representation or not). This data must satisfy (here  $D = \sum_j d_j^2$ )

$$\begin{aligned} \sum_k d_k \delta_{ijk^*} &= d_i d_j \\ \sum_{ij} d_i d_j \delta_{ijk^*} &= d_k D \end{aligned} \quad (1)$$

$j = 0$  is the unique “trivial” string type, satisfying  $0^* = 0$  and  $\delta_{0jj^*} = 1$ ,  $\delta_{0ji^*} = 0$  if  $i \neq j$ .

The Hilbert space is spanned by all configurations of all possible string types  $j$  on edges. The Hamiltonian is a sum of some mutually-commuting projectors  $H := -\sum_v \hat{Q}_v - \sum_p \hat{B}_p$  (one for each vertex  $v$  and each plaquette  $p$ ). Here each projector  $\hat{Q}_v = \delta_{ijk}$  with  $i, j, k$  on the edges incoming to the vertex  $v$ .  $\hat{Q}_v = 1$  enforces the branching rule on  $v$ . Throughout the paper we work on the subspace of states in which  $\hat{Q}_v = 1$  for all vertices. Each projector  $\hat{B}_p$  is a sum  $D^{-1} \sum_s d_s \hat{B}_p^s$  of operators that have matrix elements (on a hexagonal plaquette for example)

$$\begin{aligned} &\left\langle \begin{array}{c} j_7 \backslash j_{12} \\ j_8 \backslash j_1 \quad j_6 \backslash j_5 \\ j_2 \backslash j_3 \quad j_4 \backslash j_{11} \\ j_9 \backslash j_{10} \end{array} \middle| \hat{B}_p^s \middle| \begin{array}{c} j_7 \backslash j_{12} \\ j_8 \backslash j_1 \quad j_6 \backslash j_5 \\ j_2 \backslash j_3 \quad j_4 \backslash j_{11} \\ j_9 \backslash j_{10} \end{array} \right\rangle \\ &= v_{j_1} v_{j_2} v_{j_3} v_{j_4} v_{j_5} v_{j_6} v_{j_1'} v_{j_2'} v_{j_3'} v_{j_4'} v_{j_5'} v_{j_6'} \\ &G_{s^* j_6' j_1'}^{j_7 j_1^* j_6} G_{s^* j_1' j_2'}^{j_8 j_2^* j_1} G_{s^* j_2' j_3'}^{j_9 j_3^* j_2} G_{s^* j_3' j_4'}^{j_{10} j_4^* j_3} G_{s^* j_4' j_5'}^{j_{11} j_5^* j_4} G_{s^* j_5' j_6'}^{j_{12} j_6^* j_5} \end{aligned} \quad (2)$$

Here  $v_j = \sqrt{d_j}$  is real. The symmetrized  $6j$  symbols<sup>19</sup>  $G$  are complex numbers that satisfy

$$\begin{aligned} \text{symmetry:} & \quad G_{klm}^{ijm} = G_{nk^*l^*}^{mij} = G_{ijn^*}^{klm^*} = (G_{l^*k^*n}^{j^*i^*m^*})^* \\ \text{pentagon id:} & \quad \sum_n d_n G_{kp^*n}^{mlq} G_{mns^*}^{jip} G_{lkr^*}^{js^*n} = G_{q^*kr^*}^{jip} G_{mns^*}^{rls^*} \\ \text{orthogonality:} & \quad \sum_n d_n G_{kp^*n}^{mlq} G_{pk^*n}^{l^*m^*i^*} = \frac{\delta_{iq}}{d_i} \delta_{mlq} \delta_{k^*ip} \end{aligned} \quad (3)$$

For example, these conditions are known to be satisfied<sup>16</sup> if we take the string types  $j$  to be all irreducible representations of a finite group,  $d_j$  to be the dimension of corresponding representation space, and  $G$  to be the symmetrized Racah  $6j$  symbols for the group. In this case the LW model can be mapped<sup>26</sup> to Kitaev’s quantum double model<sup>1</sup>. More general sets of data  $\{G, d, \delta\}$  can be derived from quantum groups (or Hopf algebras)<sup>25</sup>. We will discuss such a case later using the quantum group  $SU_k(2)$  ( $k$  being the level).

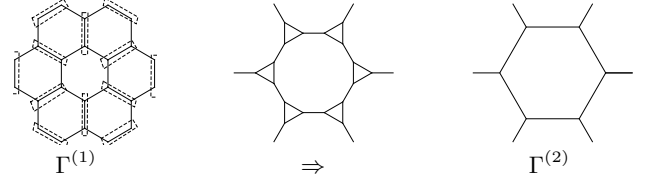


FIG. 1: Given any two trivalent graphs  $\Gamma^{(1)}$  and  $\Gamma^{(2)}$  discretizing the same surface, we can always mutate  $\Gamma^{(1)}$  to  $\Gamma^{(2)}$  by a composition of elementary  $f$  moves. In general  $\Gamma^{(1)}$  and  $\Gamma^{(2)}$  are not required to be regular lattices. These diagrams happen to be the same as<sup>28</sup>, but in a slightly different context.

### III. GROUND STATES

Any ground state  $|\Phi\rangle$  (there may be many) must be a simultaneous  $+1$  eigenvector for all projectors  $\hat{Q}_v$  and  $\hat{B}_p$ . In this section we demonstrate the topological properties of the ground states on a closed surface with non-trivial topology.

Let us begin with *any two* arbitrary trivalent graphs  $\Gamma^{(1)}$  and  $\Gamma^{(2)}$  discretizing the same surface (e.g., a torus). If we compare the LW models based on these two graphs, respectively, then immediately we see that the Hilbert spaces are quite different from each other (they have different sizes in general).

However, we may mutate between any two given trivalent graphs  $\Gamma^{(1)}$  and  $\Gamma^{(2)}$  by a composition of the following elementary moves<sup>27</sup> (see also Fig 1) :

$$\begin{aligned} f_1. & \quad \begin{array}{c} \diagup \quad \diagdown \\ \diagdown \quad \diagup \end{array} \Rightarrow \begin{array}{c} \diagup \quad \diagdown \\ \diagup \quad \diagdown \end{array}, \text{ for any edge;} \\ f_2. & \quad \begin{array}{c} \diagup \quad \diagdown \\ \diagdown \end{array} \Rightarrow \begin{array}{c} \diagup \quad \diagdown \\ \diagup \end{array}, \text{ for any vertex.} \\ f_3. & \quad \begin{array}{c} \diagup \quad \diagdown \\ \diagdown \quad \diagup \end{array} \Rightarrow \begin{array}{c} \diagup \quad \diagdown \\ \diagup \quad \diagdown \end{array}, \text{ for any triangle structure.} \end{aligned}$$

Suppose we are given a sequence of elementary  $f$  moves that connects two graphs  $\Gamma^{(1)} \rightarrow \Gamma^{(2)}$ . We now construct a linear transformation  $\mathcal{H}^{(1)} \rightarrow \mathcal{H}^{(2)}$  between the two Hilbert spaces. This is defined by associating linear maps to each elementary  $f$  move:

$$\begin{aligned} \hat{T}_1 : & \quad \left| \begin{array}{c} j_1 \backslash j_4 \\ j_2 \backslash j_5 \quad j_3 \backslash j_6 \end{array} \right\rangle \rightarrow \sum_{j_6'} v_{j_5} v_{j_5'} G_{j_3 j_4 j_5'}^{j_1 j_2 j_5} \left| \begin{array}{c} j_1 \backslash j_4 \\ j_2 \backslash j_5' \quad j_3 \backslash j_6 \end{array} \right\rangle \\ \hat{T}_2 : & \quad \left| \begin{array}{c} j_1 \backslash j_3 \\ j_2 \backslash j_6 \end{array} \right\rangle \rightarrow \sum_{j_4 j_5 j_6} \frac{v_{j_4} v_{j_5} v_{j_6}}{\sqrt{D}} G_{j_6' j_4 j_5}^{j_2 j_3 j_1} \left| \begin{array}{c} j_1 \backslash j_6' \\ j_2 \backslash j_4 \quad j_3 \backslash j_5 \end{array} \right\rangle \\ \hat{T}_3 : & \quad \left| \begin{array}{c} j_1 \backslash j_6' \\ j_2 \backslash j_4 \quad j_3 \backslash j_5 \end{array} \right\rangle \rightarrow \frac{v_{j_4} v_{j_5} v_{j_6}}{\sqrt{D}} G_{j_4' j_5' j_6}^{j_3^* j_2^* j_1^*} \left| \begin{array}{c} j_1 \backslash j_6 \\ j_2 \backslash j_4' \quad j_3 \backslash j_5' \end{array} \right\rangle \end{aligned} \quad (4)$$

The mutation transformations between  $\mathcal{H}^{(1)}$  and  $\mathcal{H}^{(2)}$  are constructed by a composition of these elementary

maps. As a special example, the operator  $\hat{B}_p = D^{-1} \sum_s d_s \hat{B}_p^s$  is such a transformation. In fact, on the particular triangle plaquette  $p$  as in (4), we have  $\hat{B}_{p=\nabla} = \hat{T}_2 \hat{T}_3$ , by using the pentagon identity in (3).

Mutation transformations are unitary on the ground states. To see this, we only need to check that the elementary maps  $\hat{T}_1$ ,  $\hat{T}_2$ , and  $\hat{T}_3$  are unitary. First note that the following relations hold:  $\hat{T}_1^\dagger = \hat{T}_1$ ,  $\hat{T}_2^\dagger = \hat{T}_3$ , and  $\hat{T}_3^\dagger = \hat{T}_2$ . We emphasize that these are maps between the Hilbert spaces on two different graphs. For example, we check  $\hat{T}_1^\dagger = \hat{T}_1$  by comparing matrix elements

$$\begin{aligned} \left\langle \begin{array}{c} j_1 \quad j_4 \\ j_2 \quad j_3 \end{array} \right| \hat{T}_1^\dagger \left| \begin{array}{c} j_1 \quad j_4 \\ j_2 \quad j_3 \end{array} \right\rangle &\equiv \left( \left\langle \begin{array}{c} j_1 \quad j_4 \\ j_2 \quad j_3 \end{array} \right| \hat{T}_1 \left| \begin{array}{c} j_1 \quad j_4 \\ j_2 \quad j_3 \end{array} \right\rangle \right)^* \\ &= v_{j_5} v_{j'_5} \left( G_{j_3 j_4 j'_5}^{j_1 j_2 j_5} \right)^* \\ &= v_{j'_5} v_{j_5} G_{j_2 j_3 j_5^*}^{j_4 j_1 j'_5} \\ &= \left\langle \begin{array}{c} j_1 \quad j_4 \\ j_2 \quad j_3 \end{array} \right| \hat{T}_1 \left| \begin{array}{c} j_1 \quad j_4 \\ j_2 \quad j_3 \end{array} \right\rangle \end{aligned} \quad (5)$$

where in the third equality we used the symmetry condition in (3).

Similarly, for  $\hat{T}_2^\dagger = \hat{T}_3$  (or  $\hat{T}_3^\dagger = \hat{T}_2$ ), we have

$$\begin{aligned} \left\langle \begin{array}{c} j_1 \quad j_3 \\ j_2 \end{array} \right| \hat{T}_2^\dagger \left| \begin{array}{c} j_1 \quad j_3 \\ j_2 \end{array} \right\rangle &\equiv \left( \left\langle \begin{array}{c} j_1 \quad j_3 \\ j_2 \end{array} \right| \hat{T}_2 \left| \begin{array}{c} j_1 \quad j_3 \\ j_2 \end{array} \right\rangle \right)^* \\ &= \frac{v_{j_4} v_{j_5} v_{j_6}}{\sqrt{D}} \left( G_{j_6^* j_4 j_5^*}^{j_2 j_3 j_1} \right)^* \\ &= \frac{v_{j_4} v_{j_5} v_{j_6}}{\sqrt{D}} G_{j_4^* j_6 j_5^*}^{j_3 j_2 j_1^*} \\ &= \left\langle \begin{array}{c} j_1 \quad j_3 \\ j_2 \end{array} \right| \hat{T}_3 \left| \begin{array}{c} j_1 \quad j_3 \\ j_2 \end{array} \right\rangle \end{aligned} \quad (6)$$

Now we verify unitarity. First,  $\hat{T}_1^\dagger \hat{T}_1 = \text{id}$  and  $\hat{T}_2^\dagger \hat{T}_2 = \hat{T}_3 \hat{T}_2 = \text{id}$  by the orthogonality condition in (3) (note that, since we have not used any information about the ground states in this argument,  $\hat{T}_1$  and  $\hat{T}_2$  are unitary on the entire Hilbert space). For unitarity of  $\hat{T}_3$  we check  $\hat{T}_3^\dagger \hat{T}_3 = \hat{T}_2 \hat{T}_3 = 1$ . The last equality only holds on the ground states since we have already seen that  $\hat{T}_2 \hat{T}_3 = \hat{B}_{p=\nabla}$  and  $\hat{B}_{p=\nabla} = 1$  only on the ground states.

As another consequence of the above relations, the Hamiltonian is hermitian since all  $\hat{B}_p$ 's consist of elementary  $\hat{T}_1$ ,  $\hat{T}_2$ , and  $\hat{T}_3$  maps. Particularly, on a triangle plaquette, we have  $\hat{B}_{p=\nabla}^\dagger = (\hat{T}_2 \hat{T}_3)^\dagger = \hat{T}_3^\dagger \hat{T}_2^\dagger = \hat{T}_2 \hat{T}_3 = \hat{B}_{p=\nabla}$ .

The mutation transformations serve as the symmetry transformations in the ground states. If  $|\Phi\rangle$  is a ground state then  $\hat{T}|\Phi\rangle$  is also a ground state, where  $\hat{T}$  is a composition of  $\hat{T}_i$ 's associated with elementary  $f$  moves from  $\Gamma^{(1)}$  to  $\Gamma^{(2)}$ . This is equivalent to the condition  $\hat{T}(\prod_p \hat{B}_p) = (\prod_{p'} \hat{B}_{p'}) \hat{T}$ , which can be verified by the

conditions in (3). (Here  $p$  and  $p'$  run over the plaquettes on  $\Gamma^{(1)}$  and  $\Gamma^{(2)}$ , respectively. Also note that the  $\hat{B}_p$ 's are mutually-commuting projectors, i.e.,  $\hat{B}_p \hat{B}_{p'} = \hat{B}_p$ , and thus  $\prod_p \hat{B}_p$  is the projector that projects onto the ground states.)

These symmetry transformations look a little different from the usual ones since they may transform between the Hilbert spaces  $\mathcal{H}^{(1)}$  and  $\mathcal{H}^{(2)}$  on two different graphs  $\Gamma^{(1)}$  and  $\Gamma^{(2)}$ . In general,  $\Gamma^{(1)}$  and  $\Gamma^{(2)}$  do not have the same number of vertices and edges. And thus  $\mathcal{H}^{(1)}$  and  $\mathcal{H}^{(2)}$  have different sizes. However, if we restrict to the ground-state subspaces  $\mathcal{H}_0^{(1)}$  and  $\mathcal{H}_0^{(2)}$ , mutation transformations are invertible. In fact, they are unitary as we have just shown.

The tensor equations on the  $6j$  symbols in (3) give rise to a simple result: each mutation that preserves the spatial topology of the two graphs induces a unitary symmetry transformation. During the mutations, local structures of the graphs are destroyed, while the spatial topology of the graphs is not changed. Correspondingly, the local information of the ground states may be lost, while the topological feature of the ground states is preserved. In fact, any topological feature can be specified by a topological observable  $\hat{O}$  that is invariant under all mutation transformations  $\hat{T}$  from  $\mathcal{H}^{(1)}$  to  $\mathcal{H}^{(2)}$ :  $\hat{O}' \hat{T} = \hat{T} \hat{O}$  (where  $\hat{O}$  is defined on the graph  $\Gamma^{(1)}$  and  $\hat{O}'$  on  $\Gamma^{(2)}$ ).

The symmetry transformations provides a way to characterize the topological phase by a topological observable. In the next section we will investigate the GSD as such an observable.

Let us end this section by remarking on uniqueness of the mutation transformations. There may be many ways to mutate  $\Gamma^{(1)}$  to  $\Gamma^{(2)}$  using  $f_1$ ,  $f_2$  and  $f_3$  moves. Each way determines a corresponding transformation between the Hilbert spaces of ground states,  $\mathcal{H}_0^{(1)}$  and  $\mathcal{H}_0^{(2)}$ . It turns out that all these transformations are actually the same if the initial and final graphs  $\Gamma^{(1)}$  to  $\Gamma^{(2)}$  are fixed, i.e., independent of which way we choose to mutate the graph  $\Gamma^{(1)}$  to  $\Gamma^{(2)}$ . This means that the ground state Hilbert spaces on different graphs can be identified (up to a mutation transformation) and all graphs are equally good.

One consequence of the uniqueness of the mutation transformation is that the degrees of freedom in the ground states do not depend on the specific structure of the graph. In this sense, the LW model is the Hamiltonian version of some discrete TQFT (actually, Turaev-Viro type TQFT, see<sup>21</sup>). The fact that the degrees of freedom of the ground states depend only on the topology of the closed surface  $M$  is a typical characteristic of topological phases<sup>7-9,12,15</sup>.

#### IV. GROUND STATE DEGENERACY

In this section we investigate the simplest nontrivial topological observable, the GSD. Since  $\prod_p \hat{B}_p$  is the pro-

jector that projects onto the ground states, taking a trace computes  $\text{GSD} = \text{tr}(\prod_p \hat{B}_p)$ .

We can show that GSD is a topological invariant. Namely, in the previous section we mentioned that, by using (3),  $\prod_p \hat{B}_p$  is invariant under any mutation  $\hat{T}$  between the Hilbert spaces  $\mathcal{H}^{(1)}$  and  $\mathcal{H}^{(2)}$ :  $\hat{T}^\dagger(\prod_{p'} \hat{B}_{p'})\hat{T} = \prod_p \hat{B}_p$ . Taking a trace of both sides leads to  $\text{tr}'(\prod_{p'} \hat{B}_{p'}) = \text{tr}(\prod_p \hat{B}_p)$ , where the traces are evaluated on  $\mathcal{H}^{(2)}$  and  $\mathcal{H}^{(1)}$  respectively.

The independence of the GSD on the local structure of the graphs provides a practical algorithm for computing the GSD, since we may always use the simplest graph (see Fig 2 and examples in the next section).

Expanding the GSD explicitly in terms of  $6j$  symbols using (2) we obtain

$$\begin{aligned} \text{GSD} &= \sum_{j_1 j_2 j_3 j_4 j_5 j_6 \dots} \left\langle \begin{array}{c} j_1 \quad j_5 \quad j_4 \\ j_2 \quad \quad j_3 \end{array} \right\rangle \left( \prod_p \hat{B}_p \right) \left\langle \begin{array}{c} j_1 \quad j_5 \quad j_4 \\ j_2 \quad \quad j_3 \end{array} \right\rangle \\ &= D^{-P} \sum_{s_1 s_2 s_3 s_4 \dots} d_{s_1} d_{s_2} d_{s_3} d_{s_4} \dots \\ &\quad \sum_{j'_1 j'_2 j'_3 j'_4 j'_5 \dots} d_{j'_1} d_{j'_2} d_{j'_3} d_{j'_4} d_{j'_5} \dots \sum_{j_1 j_2 j_3 j_4 j_5 \dots} d_{j_1} d_{j_2} d_{j_3} d_{j_4} d_{j_5} \dots \\ &\quad \left( G_{s_1^* j'_1 j'_5}^{j_2 j_5 j_1} G_{s_2^* j'_2 j'_5}^{j'_1 j_2 j'_5} G_{s_3^* j'_3 j'_2}^{j_5 j'_1 j'_2} \right) \left( G_{s_1^* j'_5 j'_4}^{j_3 j_4 j'_5} G_{s_2^* j'_3 j'_5}^{j'_4 j'_5 j_3} G_{s_4^* j_4 j_3}^{j'_5 j'_3 j'_4} \right) \dots \end{aligned} \quad (7)$$

The formula needs some explanation.  $P$  is the total number of plaquettes of the graph. Each plaquette  $p$  contributes a summation over  $s_p$  together with a factor of  $\frac{d_{s_p}}{D}$ . In the picture in (7) the top plaquette is being operated on first by  $\hat{B}_{p_1}^{s_1}$ , next the bottom plaquette by  $\hat{B}_{p_2}^{s_2}$ , third the left plaquette by  $\hat{B}_{p_3}^{s_3}$ , and finally the right plaquette by  $\hat{B}_{p_4}^{s_4}$ . Although ordering of the  $\hat{B}_p^s$  operators is not important (since all  $\hat{B}_p^s$  commute with each other), it is important to make an ordering choice (for all plaquettes on the graph) *once and for all*.

Each edge  $e$  contributes a summation over  $j_e$  and  $j'_e$  together with a factor of  $d_{j_e} d_{j'_e}$ . Each vertex contributes three  $6j$  symbols.

The indices on the  $6j$  symbols work as follows: since each vertex borders three plaquettes where  $\hat{B}_p^s$ 's are being applied, we pick up a  $6j$  symbol for each corner. However, ordering is important: because we have an overall ordering of  $\hat{B}_p^s$ 's, at each vertex we get an induced ordering for the  $6j$  symbols. Starting with the  $6j$  symbol furthest left we have no primes on the top row. The bottom two indices pick up primes. All of these variables (primed or not) are fed into the next  $6j$  symbol and the same rule applies: the bottom two indices pick up a prime with the convention  $()'' = ()$ .

By the calculation of the GSD, we have characterized a topological property of the phase using local quantities living on a graph discretizing  $M$  of nontrivial topology.

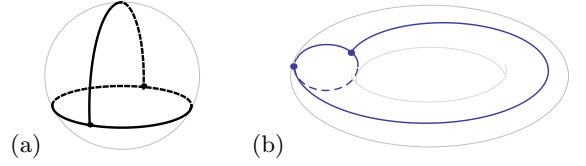


FIG. 2: All trivalent graphs can be reduced to their simplest structures by compositions of elementary  $f$  moves. (a) on a sphere: 2 vertices, 3 edges, and 3 plaquettes. (b) on a torus: 2 vertices, 3 edges, and 1 plaquette.

## V. EXAMPLES

(1) *On a sphere.* To calculate the GSD, we need to input the data  $\{G_{klm}^{ijm}, d_j, \delta_{ijm}\}$  and evaluate the trace in (7). We start by computing the GSD in the simplest case of a sphere.

Let's consider the simplest graph as in Fig. 2(a). We show in Appendix A that the ground state is non-degenerate on the sphere without referring to any specific structure in the model:  $\text{GSD}^{\text{sphere}} = 1$ . In fact, for more general graphs one can write down<sup>28</sup> the ground state as  $\prod_p \hat{B}_p |0\rangle$  up to a normalization factor, where in  $|0\rangle$  all edges are labeled by string type 0.

We notice that the GSD on the open disk (which is topologically the same as the 2d plane) can be studied using the same technique. This is because the open disk can be obtained by puncturing the sphere in Fig 2(a) at the bottom. Although this destroys the bottom plaquette, we notice that the constraint  $\hat{B}_p = 1$  from the bottom plaquette is automatically satisfied as a consequence of the same constraint on all other plaquettes. The fact that  $\text{GSD}^{\text{sphere}} (= \text{GSD}^{\text{disk}}) = 1$  indicates the non-chiral topological order in the LW model.

(2) *Quantum double model.* When the data are determined by representations of a finite group  $G$ , the LW model is mapped to Kitaev's quantum double model<sup>1,26</sup>. The ground states corresponds one-to-one to the flat  $G$ -connections<sup>1</sup>. The GSD is

$$\text{GSD}_{\text{QD}} = \left| \frac{\text{Hom}(\pi_1(M), G)}{G} \right| \quad (8)$$

where  $\text{Hom}(\pi_1(M), G)$  is the space of homomorphisms from the fundamental group  $\pi_1(M)$  to  $G$ , and  $G$  in the quotient acts on this space by conjugation.

In particular, the GSD (8) on a torus is

$$\text{GSD}_{\text{QD}}^{\text{torus}} = |\{(a, b) | a, b \in G; aba^{-1}b^{-1} = e\} / \sim| \quad (9)$$

where  $\sim$  in the quotient is the equivalence by conjugation,

$$(a, b) \sim (hah^{-1}, h b h^{-1}) \quad \text{for all } h \in G$$

The number (9) is also the total number of irreducible representations<sup>31</sup> of the quantum double  $D(G)$  of the group  $G$ . On the other hand, the quasiparticles in the model are classified<sup>1</sup> by the quantum double  $D(G)$ . Thus



the GSD on a torus is equal to the number of particle species in this example.

(3)  $SU_k(2)$  structure on a torus. More generally, on a torus any trivalent graph can be reduced to the simplest one with two vertices and three edges, as in Fig 2(b). On this graph the GSD consists of six local  $6j$  symbols.

$$\text{GSD} = D^{-1} \sum_{sj_1 j_2 j_3 j'_1 j'_2 j'_3} d_s d_{j_1} d_{j_2} d_{j_3} d_{j'_1} d_{j'_2} d_{j'_3} \left( G_{sj_3^* j_2^*}^{j_1 j_2 j_3^*} G_{sj_2 j_1^*}^{j_3^* j_1^* j_2^*} G_{sj_1 j_3^*}^{j_2^* j_2^* j_1^*} \right) \left( G_{sj_1^* j_3^*}^{j_2^* j_2^* j_1^*} G_{sj_2^* j_1^*}^{j_3^* j_3^* j_2^*} G_{sj_3^* j_2^*}^{j_1^* j_1^* j_3^*} \right) \quad (10)$$

Now let us take the example using the quantum group  $SU_k(2)$ . It is known that  $SU_k(2)$  has  $k+1$  irreducible representations, and thus the GSD we calculate is finite. We take the string types to be these representations, labeled as  $0, 1, \dots, k$ , and the data  $\{G_{klm}^{ijm}, d_j, \delta_{ijm}\}$  to be determined by these representations (for more details, see<sup>24,29,30</sup>).

In Appendix B we show that in this case (for the LW model on a torus with string types given by irreps of  $SU_k(2)$ ) we have  $\text{GSD} = (k+1)^2$ . We argue this both analytically and numerically.

On the other hand, it is widely believed that when the string types in the LW model are irreps from a quantum group at level  $k$ , then the associated TQFT is given by doubled Chern-Simons theory associated with the corresponding Lie group at level  $\pm k$ <sup>24,32</sup>. This equivalence tells us that in this case the LW model can be viewed as a Hamiltonian realization of the doubled Chern-Simons theory on a lattice, and it provides an explicit picture of how the LW model describes doubled topological phases.

Along these lines, our result is consistent<sup>33</sup> with the result  $\text{GSD}_{CS} = k+1$  for Chern-Simons  $SU(2)$  theory at level  $k$  on a torus. This can be seen since the Hilbert space associated to doubled Chern-Simons should be the tensor product of two copies of Chern-Simons theory at level  $\pm k$ .

## VI. SUMMARY AND DISCUSSIONS

In this paper, we studied the LW model that describes 2d topological phases which do not break time-reversal symmetry. By examining the 2d (trivalent) graphs with same topology which are related to each other by a given finite set of operations (Pachner moves), we developed techniques to deal with topological properties of the ground states. Using them, we have been able to show explicitly that the GSD is determined only by the topology of the surface the system lives on, which is a typical feature of topological phases. We also demonstrated how to obtain the GSD from local data in a general way. We explicitly showed that the ground state of any LW Hamiltonian on a sphere is non-degenerate. Moreover, the LW model associated with quantum group  $SU_k(2)$  was studied, and our result for the GSD on a torus is

consistent with the conjecture that the LW model associated with quantum group is the realization of a doubled Chern-Simons theory on a lattice or discrete graph.

Finally, let us indicate possible extension of the results to more general cases. First, more generally in the LW model, an extra discrete degree of freedom, labelled by an index  $\alpha$ , may be put on the vertices. Then the branching rule  $\delta_{ijk}^\alpha$ , when its value is 1, may carry an extra index  $\alpha$ . (In representation language this implies that given irreducible representations  $i, j$  and  $k$ , there may be multiple inequivalent ways to obtain the trivial representation from the tensor product of  $i \otimes j \otimes k$ . The index  $\alpha$  just labels these different ways.) The  $6j$  symbols accordingly carry more indices. (For more details see the first Appendix in the original paper<sup>16</sup> of the LW model.) The expression (7) for GSD is expected to be generalizable to these cases. Secondly, the spatial manifold (e.g. a torus) on which the graph is defined may carry non-trivial charge, e.g. labelled by  $i\bar{i}$  in the  $SU_k(2)$  case. This corresponds to having a so-called fluxon excitation (of type  $i\bar{i}$ ) above the original LW ground states. The lowest states of this subsector in the LW model coincide with the ground states for the Hamiltonian obtained by replacing the plaquette projector  $\hat{B}_p = D^{-1} \sum_j d_j \hat{B}_p^j$  with  $\hat{B}_p = D^{-1} \sum_j s_{ij} \hat{B}_p^j$ , where  $s_{ij}$  is the modular  $S$ -matrix. (See Appendix B.) The GSD in this case is computable too, but we leave this for a future paper<sup>34</sup>.

## Acknowledgments

YH thanks Department of Physics, Fudan University for warm hospitality he received during a visit in summer 2010. YSW was supported in part by US NSF through grant No. PHY-0756958, No. PHY-1068558 and by FQXi.

## Appendix A: GSD = 1 on a sphere

In appendix, we derive  $\text{GSD} = 1$  on a sphere for a general Levin-Wen model, without referring to any specific structure of the data  $\{d, \delta, G\}$ . All we will use in the derivation are the general properties in eq. (1) and eq. (3).

The simplest trivalent graph on a sphere has three plaquettes and three edges, as illustrated in Fig. 2(a). Following the standard procedure as in (7), the GSD is

expanded as

$$\begin{aligned}
\text{GSD}^{\text{sphere}} &= \sum_{j_1 j_2 j_3} \left\langle \left( \begin{array}{c} j_1 \\ \leftarrow j_3 \rightarrow \\ j_2 \end{array} \right) \left| \hat{B}_{p_2} \hat{B}_{p_3} \hat{B}_{p_1} \right| \left( \begin{array}{c} j_1 \\ \leftarrow j_3 \rightarrow \\ j_2 \end{array} \right) \right\rangle \\
&= \sum_{j_1 j_2 j_3} \left\langle \left( \begin{array}{c} j_1 \\ \leftarrow j_3 \rightarrow \\ j_2 \end{array} \right) \left| \frac{1}{D} \sum_t d_t \hat{B}_{p_2}^t \right. \right. \\
&\quad \left. \frac{1}{D} \sum_s d_s \hat{B}_{p_3}^s \frac{1}{D} \sum_r d_r \hat{B}_{p_1}^r \left| \left( \begin{array}{c} j_1 \\ \leftarrow j_3 \rightarrow \\ j_2 \end{array} \right) \right. \right\rangle \\
&= \sum_{j_1 j_2 j_3 j'_1 j'_2 j'_3} \frac{1}{D} \sum_r d_r v_{j_1} v_{j_3} v_{j'_1} v_{j'_3} G_{r^* j'_1^* j'_3}^{j_2^* j_3 j_1^*} G_{r^* j'_3^* j'_1^*}^{j_2 j_1 j_3^*} \\
&\quad \frac{1}{D} \sum_s d_s v_{j'_1} v_{j_2} v_{j_1} v_{j'_2} G_{s^* j'_2^* j'_1^*}^{j_3 j'_1^* j_2^*} G_{s^* j'_1^* j'_2^*}^{j_3 j_2 j_1^*} \\
&\quad \frac{1}{D} \sum_t d_t v_{j'_2} v_{j'_3} v_{j_2} v_{j_3} G_{t^* j_3 j_2^*}^{j_1^* j'_2^* j'_3} G_{t^* j_2 j_3^*}^{j_1 j'_3 j'_2} \quad (\text{A1})
\end{aligned}$$

where  $\hat{B}_{p_1}$  is acting on the top bubble plaquette,  $\hat{B}_{p_2}$  on the bottom bubble plaquette, and  $\hat{B}_{p_3}$  on the rest plaquette outside the two bubbles.

All  $6j$  symbols can be eliminated by using the orthogonality condition in eq. (3) three times,

$$\begin{aligned}
\sum_r d_r G_{r^* j'_1^* j'_3}^{j_2^* j_3 j_1^*} G_{r^* j'_3^* j'_1^*}^{j_2 j_1 j_3^*} &= \frac{1}{d_{j_2}} \delta_{j'_1 j_2 j'_3}^* \delta_{j_1 j_2 j_3^*} \\
\sum_s d_s G_{s^* j'_2^* j'_1^*}^{j_3 j'_1^* j_2^*} G_{s^* j'_1^* j'_2^*}^{j_3 j_2 j_1^*} &= \frac{1}{d_{j'_3}} \delta_{j'_1 j_2 j'_3}^* \delta_{j_1 j'_2 j'_3^*} \\
\sum_t d_t G_{t^* j_3 j_2^*}^{j_1^* j'_2^* j'_3} G_{t^* j_2 j_3^*}^{j_1 j'_3 j'_2} &= \frac{1}{d_{j_1}} \delta_{j_1 j_2 j_3^*} \delta_{j_1 j'_2 j'_3^*} \quad (\text{A2})
\end{aligned}$$

and the GSD is a summation in terms of  $\{d, \delta\}$ :

$$\text{GSD}^{\text{sphere}} = \frac{1}{D^3} \sum_{j_1 j_2 j_3 j'_1 j'_2 j'_3} d_{j'_1} d_{j'_2} d_{j_3} \delta_{j_1 j_2 j_3^*} \delta_{j'_1 j_2 j'_3}^* \delta_{j_1 j'_2 j'_3^*} \quad (\text{A3})$$

Summing over  $j'_1, j'_2$ , and  $j_3$  using (1) finally leads to  $\text{GSD}^{\text{sphere}} = 1$ .

## Appendix B: GSD on a torus for $SU_k(2)$

Let us consider the example associated with the quantum group  $SU_k(2)$  (with the level  $k$  an positive integer) and calculate the GSD on a torus.

There are  $k+1$  string types, labeled as  $j = 0, 1, 2, \dots, k$ . They are the irreducible representations of  $SU_k(2)$ . The quantum dimensions  $d_j$  are required to be positive for all  $j$ , in order that the Hamiltonian is hermitian. Explicitly,

they are

$$\begin{aligned}
d_j &= \frac{\sin \frac{(j+1)\pi}{k+2}}{\sin \frac{\pi}{k+2}} \\
D &= \sum_{j=0}^k d_j^2 = \frac{k+2}{2 \sin^2 \frac{\pi}{k+2}} \quad (\text{B1})
\end{aligned}$$

The branching rule is  $\delta_{rst} = 1$  if

$$\begin{cases} r + s + t \text{ is even} \\ r + s \geq t, s + t \geq r, t + r \geq s \\ r + s + t \leq 2k \end{cases} \quad (\text{B2})$$

and  $\delta_{rst} = 0$  otherwise. The explicit formula for the  $6j$  symbol can be found in<sup>29,30</sup>. However, we do not need the detailed data of the  $6j$  symbol in the following computation of the GSD.

Let us start with formula in (10), and reorder the  $6j$  symbols,

$$\begin{aligned}
\text{GSD} &= D^{-1} \sum_{s j_1 j_2 j_3 j'_1 j'_2 j'_3} d_s \left( v_{j_1} v_{j_3} v_{j'_1} v_{j'_3} G_{s^* j'_1^* j'_3}^{j_2^* j_3 j_1^*} G_{s^* j'_3^* j'_1^*}^{j_2 j_1 j_3^*} \right) \\
&\quad \left( v_{j'_1} v_{j_2} v_{j_1} v_{j'_2} G_{s^* j'_2^* j'_1^*}^{j_3 j'_1^* j_2^*} G_{s^* j'_1^* j'_2^*}^{j_3 j_2 j_1^*} \right) \\
&\quad \left( v_{j'_2} v_{j'_3} v_{j_2} v_{j_3} G_{s^* j_3 j_2^*}^{j_1^* j'_2^* j'_3} G_{s^* j_2 j_3^*}^{j_1 j'_3 j'_2} \right) \\
&= D^{-1} \sum_{s j_1 j_2 j_3 j'_1 j'_2 j'_3} d_s \left( v_{j_1} v_{j_3} v_{j'_1} v_{j'_3} G_{s^* j'_1^* j'_3}^{j_2^* j_3 j_1^*} G_{s j'_3 j'_1^*}^{j_2 j_1 j_3^*} \right) \\
&\quad \left( v_{j'_1} v_{j_2} v_{j_1} v_{j'_2} G_{s^* j'_2^* j'_1^*}^{j_3 j'_1^* j_2^*} G_{s j'_1^* j'_2^*}^{j_3 j_2 j_1^*} \right) \\
&\quad \left( v_{j'_2} v_{j'_3} v_{j_2} v_{j_3} G_{s^* j_3 j_2^*}^{j_1^* j'_2^* j'_3} G_{s j_2 j_3^*}^{j_1 j'_3 j'_2} \right) \quad (\text{B3})
\end{aligned}$$

where the symmetry condition in (3) was used in the second equality.

Let us compare the formula in (B3) with that in (A1). We set  $j = j^*$  for all  $j$  and drop all stars, since all irreducible representations of  $SU_k(2)$  are self-dual. Then we find that the summation (B3) has the same form as the trace of  $D^{-1} \sum_s d_s \hat{B}_{p_2}^s \hat{B}_{p_3}^s \hat{B}_{p_1}^s$  on the graph on a sphere as in (A1),

$$\begin{aligned}
&\text{tr}^{\text{torus}} \left( \frac{1}{D} \sum_s d_s \hat{B}_p^s \right) \\
&= \sum_{j_1 j_2 j_3} \left\langle \left( \begin{array}{c} j_1 \\ \leftarrow j_3 \rightarrow \\ j_2 \end{array} \right) \left| \frac{1}{D} \sum_s d_s \hat{B}_{p_2}^s \hat{B}_{p_3}^s \hat{B}_{p_1}^s \right| \left( \begin{array}{c} j_1 \\ \leftarrow j_3 \rightarrow \\ j_2 \end{array} \right) \right\rangle \\
&= \text{tr}^{\text{sphere}} \left( \frac{1}{D} \sum_s d_s \hat{B}_{p_2}^s \hat{B}_{p_3}^s \hat{B}_{p_1}^s \right) \quad (\text{B4})
\end{aligned}$$

where  $\hat{B}_p^s$  is defined on the only plaquette  $p$  on the torus (see Fig. 2(b)), while  $\hat{B}_{p_1}^s \hat{B}_{p_2}^s \hat{B}_{p_3}^s$  is defined on the same graph on a sphere as in (A1) (see Fig. 2(a)).

The GSD on a torus becomes a trace on a sphere. The latter is easier to deal with since the ground state on a

sphere is non-degenerate. The counting of ground states on a torus turns into a problem dealing with excitations on the sphere.

In the following we evaluate the summation in the representation of elementary excitations. let us introduce a new set of operators  $\{\hat{n}_p^r\}$  by a transformation,

$$\hat{n}_p^r = \sum_s s_{r0} s_{rs} \hat{B}_p^s, \quad \hat{B}_p^s = \sum_r \frac{s_{rs}}{s_{r0}} \hat{n}_p^r \quad (\text{B5})$$

Here  $s_{rs}$  is a symmetric matrix (referred to as the modular  $S$ -matrix for  $SU_k(2)$ ),

$$s_{rs} = \frac{1}{\sqrt{D}} \frac{\sin \frac{(r+1)(s+1)\pi}{k+2}}{\sin \frac{\pi}{k+2}} \quad (\text{B6})$$

and has the properties

$$\begin{aligned} s_{rs} &= s_{sr}, \quad s_{r0} = d_r / \sqrt{D} \\ \sum_s s_{rs} s_{st} &= \delta_{rt} \\ \sum_w \frac{s_{wr} s_{ws} s_{wt}}{s_{w0}} &= \delta_{rst} \end{aligned} \quad (\text{B7})$$

Eq. (B5) can be viewed as a finite discrete Fourier transformation between  $\{\hat{n}_p^r\}$  and  $\{\hat{B}_p^s\}$ . By properties (B7), we see that  $\{\hat{n}_p^r\}$  are mutually orthonormal projectors, and they form a resolution of the identity:

$$\hat{n}_p^r \hat{n}_p^s = \delta_{rs} \hat{n}_p^r, \quad \sum_r \hat{n}_p^r = \text{id} \quad (\text{B8})$$

In particular,  $\hat{n}_p^0 = \frac{1}{D} \sum_s d_s \hat{B}_p^s$  is the operator  $\hat{B}_p$  in the Hamiltonian. The operator  $\hat{n}_p^r$  projects onto the states with a quasiparticle (labeled by  $r$  type) occupying the plaquette  $p$ . Expressed as common eigenvectors of  $\{\hat{n}_p^r\}$ , the elementary excitations are classified by the configuration of these quasiparticles.

Particularly, on the graph on a sphere as in (B4), the Hilbert space has a basis of  $\{|r_1, r_2, r_3\rangle\}$ , where only those  $r_1, r_2$ , and  $r_3$  that satisfy  $\delta_{r_1 r_2 r_3} = 1$  are allowed. Each basis vector  $|r_1, r_2, r_3\rangle$  is an elementary excitation with the quasiparticles labeled by  $r_1, r_2$ , and  $r_3$  occupying the plaquettes  $p_1, p_2$ , and  $p_3$ . The configuration of quasiparticles are globally constrained by  $\delta_{r_1 r_2 r_3} = 1^{34}$ . Therefore, tracing operators  $\{\hat{n}_p^r\}$  leads to

$$\text{tr}(\hat{n}_{p_2}^{r_2} \hat{n}_{p_3}^{r_3} \hat{n}_{p_1}^{r_1}) = \delta_{r_2 r_3 r_1} \quad (\text{B9})$$

Applying this rule reduces the summation (B4) to

$$\begin{aligned} & \text{tr}\left(\frac{1}{D} \sum_s d_s \hat{B}_{p_2}^s \hat{B}_{p_3}^s \hat{B}_{p_1}^s\right) \\ &= \text{tr}\left(\frac{1}{D} \sum_s d_s \sum_{r_1 r_2 r_3} \frac{s_{sr_1} s_{sr_2} s_{sr_3}}{s_{r_1 0} s_{r_2 0} s_{r_3 0}} \hat{n}_{p_2}^{r_2} \hat{n}_{p_3}^{r_3} \hat{n}_{p_1}^{r_1}\right) \\ &= \sum_{r_1 r_2 r_3} \frac{1}{D} \sum_s d_s \frac{s_{sr_1} s_{sr_2} s_{sr_3}}{s_{r_1 0} s_{r_2 0} s_{r_3 0}} \delta_{r_1 r_2 r_3} \end{aligned} \quad (\text{B10})$$

Then we substitute (B1), (B2) and (B6) in and obtain

$$\begin{aligned} \text{GSD}_{SU_k(2)}^{\text{torus}} &= \sum_{r_1, r_2, r_3=0}^k \frac{\sin \frac{\pi}{k+2} \delta_{r_1+r_2+r_3, 2k}}{\sin \frac{(r_1+1)\pi}{k+2} \sin \frac{(r_2+1)\pi}{k+2} \sin \frac{(r_3+1)\pi}{k+2}} \\ &= \sum_{r=0}^k \sum_{s=0}^r \frac{\sin \frac{\pi}{k+2}}{\sin \frac{(r+1)\pi}{k+2} \sin \frac{(s+1)\pi}{k+2} \sin \frac{(r-s+1)\pi}{k+2}} \\ &= (k+1)^2. \end{aligned} \quad (\text{B11})$$

(Here we omit a rigorous proof of the last equality.)

We can also verify  $\text{GSD} = (k+1)^2$  by a direct numerical computation. We take the approach in<sup>30</sup> to construct the numerical data of  $6j$  symbols. The construction depends on a parameter, the Kauffman variable  $A$  (in the same convention as in<sup>30</sup>), which is specialized to roots of unity. We make the following choice:

$$\begin{cases} A = \exp(\pi i/3) & \text{at } k = 1 \\ A = \exp(3\pi i/8) & \text{at } k = 2 \\ A = \exp(3\pi i/5) & \text{at } k = 3 \end{cases} \quad (\text{B12})$$

By this choice, the quantum dimensions  $d_j$  take the values as in (B1), and the  $6j$  symbols satisfy the self-consistent conditions in (3). Using such data of quantum dimensions  $d_j$  and  $6j$  symbols, We compute the summation (10) at

$$\begin{cases} \text{GSD} = 4 & \text{at } k = 1 \\ \text{GSD} = 9 & \text{at } k = 2 \\ \text{GSD} = 16 & \text{at } k = 3 \end{cases} \quad (\text{B13})$$

which verifies  $\text{GSD} = (k+1)^2$  in the particular cases.



- 
- \* Electronic address: [yuting@physics.utah.edu](mailto:yuting@physics.utah.edu)  
† Electronic address: [stirling@physics.utah.edu](mailto:stirling@physics.utah.edu)  
‡ Electronic address: [wu@physics.utah.edu](mailto:wu@physics.utah.edu)
- <sup>1</sup> A. Yu. Kitaev, *Annals Phys.* **303**, 2-30(2003).
  - <sup>2</sup> M. H. Freedman, A. Kitaev, M. Larsen, Z.H. Wang, [arXiv:quant-ph/0101025](https://arxiv.org/abs/quant-ph/0101025).
  - <sup>3</sup> C. Nayak, S. H. Simon, A. Stern, M. Freedman, S. Das Sarma, *Rev. Mod. Phys.* **80**, 1083 (2008).
  - <sup>4</sup> Z. Wang, *Topological Quantum Computation*, CBMS No. 112, American Mathematical Society, U.S. (2010).
  - <sup>5</sup> S.C. Zhang, T.H. Hansson, S. Kivelson, *Phys. Rev. Lett.* **62**, 82 (1989); X.G. Wen and A. Zee, *Phys. Rev. Lett.* **69**, 1811 (1992).
  - <sup>6</sup> E. Witten, *Comm. Math. Phys.* **121**, 351 (1989).
  - <sup>7</sup> R. Tao, Y.S. Wu, *Phys. Rev. B* **30**, 1907 (1984).
  - <sup>8</sup> Q. Niu, D. J. Thouless, Y.S. Wu, *Phys. Rev. B* **31**, 3372 (1985).
  - <sup>9</sup> X.G. Wen, Q. Niu, *Phys. Rev. B* **41**, 9377 (1990).
  - <sup>10</sup> Y. Hatsugai, M. Kohmoto, Y.S. Wu, *Phys. Rev. Lett.* **66**, 659 (1991).
  - <sup>11</sup> Y. Hatsugai, M. Kohmoto, Y.S. Wu, *Phys. Rev. B* **43**, 10761 (1991).
  - <sup>12</sup> M. Sato, M. Kohmoto, Y.S. Wu, *Phys. Rev. Lett.* **97**, 010601 (2006).
  - <sup>13</sup> F. Wilczek, *Phys. Rev. Lett.* **48**, 1144 (1982).
  - <sup>14</sup> Y.S. Wu, *Phys. Rev. Lett.* **52**, 2103 (1984).
  - <sup>15</sup> X.G. Wen, A. Zee, *Phys. Rev. B* **44**, 274 (1991).
  - <sup>16</sup> M. Levin, X.G. Wen, *Phys. Rev. B* **71**, 045110 (2005).
  - <sup>17</sup> X.G. Wen, *Phys. Rev. B* **68**, 115413 (2003); *Phys. Rev. D* **68**, 065003 (2003).
  - <sup>18</sup> X. Chen, Z.C. Gu, X.G. Wen, *Phys. Rev. B* **82**, 155138 (2010).
  - <sup>19</sup> Xiao-Gang Wen, *Tensor category theory of string-net condensation*, <http://dao.mit.edu/~wen/>.
  - <sup>20</sup> V. G. Turaev, *Quantum Invariants of Knots and 3-manifolds*, Walter de Gruyter, Berlin, (1994).
  - <sup>21</sup> Z. Kádár, A. Marzuoli and M. Rasetti, *Int. J. Quant. Inf.* **7**, suppl. 195-203(2009).
  - <sup>22</sup> M. Freedman, C. Nayak, K. Shtengel, Walker, Z. Wang, *Ann. Phys.* **310**, 428 (2004).
  - <sup>23</sup> F. Burnell, S. Simon, *New J. Phys.* **13**, 065001 (2011).
  - <sup>24</sup> N. Reshetikhin, V. G. Turaev, *Invent. Math.* **103**, 547 (1991).
  - <sup>25</sup> C. Kassel, *Quantum Groups*, Springer GTM (1994).
  - <sup>26</sup> O. Buerschaper, M. Aguado, *Phys. Rev. B* **80**, 155136 (2009).
  - <sup>27</sup> U. Pachner, *Arch. Math.* **30**, 89-98 (1978); in a slightly different context.
  - <sup>28</sup> Z. Gu, M. Levin, B. Swingle, X.-G. Wen, *Phys. Rev. B* **79**, 085118 (2009).
  - <sup>29</sup> A. Kirillov and N. Reshetikhin, *Representations of the algebra  $U_q(sl(2))$ ,  $q$ -orthogonal polynomials and invariants of links*, in V.G. Kac, ed., *Infinite dimensional Lie algebras and groups*, *Proceedings of the conference held at CIRM, Luminy, Marseille*, p. 285, World Scientific, Singapore (1988).
  - <sup>30</sup> G. Masbaum, P. Vogel, *Pacific J. Math* **164** No. 2 (1994).
  - <sup>31</sup> R. Dijkgraaf, V. Pasquier and P. Roche, *Nucl. Phys. B (Proc. Suppl.)* **18B**, 60(1990).
  - <sup>32</sup> E. Witten, *Nucl. Phys. B* **311**, 46 (1988).
  - <sup>33</sup> X.G. Wen and A. Zee, *Phys. Rev. B* **58**, 15717 (1998).
  - <sup>34</sup> Y. Hu, S. Stirling and Y.S. Wu (in preparation).